BESO Approach for the Optimal Retrofitting Design of Steel Hollow-Section Columns Supporting Industry Cranes

***Rut Su[1], Thu Huynh Van[1] and †Sawekchai Tangaramvong[1]**

[1]Applied Mechanics and Structures Research Unit, Department of Civil Engineering, Chulalongkorn University, Bangkok 10330, Thailand.

*Presenting author: rut-zu@hotmail.com
†Corresponding author: sawekchai.t@chula.ac.th

Abstract

The local buckling phenomenon presents one of the main premature failures often prohibiting the steel hollow-section columns to attend the ultimate strength capacity. A strengthening method is then required to extend the service life of the member. This paper presents the optimal retrofitting design of standard steel hollow-section columns using external steel plates, such that the ultimate strength of the post-retrofitted column sufficiently resists the design load imposed by an industrial crane. The optimal design adopts a so-called bi-directional evolutionary structural optimization (BESO) algorithm that determines the cost-effective distribution of steel plate topology welded to the column. The proposed method realistically considers the influences of inelastic material properties and geometric nonlinearity, simultaneously. The BESO algorithm is encoded within the MATLAB modeling framework providing a direct application interface to ANSYS (a commercial-purposed finite element analysis software), which models the retrofitting joint between steel column and corbel using the comprehensive 3D finite elements. The robustness of the proposed scheme is illustrated through standard steel warehouse applications. The accuracy and integrity of the resulting design are validated by the full elastoplastic responses of the post-retrofitted column under applied forces.

Keywords: Local Buckling Failure; Topology Optimization; Evolutionary Structural Optimization; Column Retrofitting Design; Nonlinear Finite Element Analysis.

1. Introduction

Steel structural design is a combination process between architecture, safety and integrity. Good design complies with various performance criteria posed by all stakeholders at optimal resources. The design of hollow steel section (HSS) members has gained the popularity from designers. In views of strength consideration, the HSS provides the higher load capacity than the open sections [1]. Such physical property has made the HSS suitable for various structures and infrastructures, especially those with the special requirement on a long-span capability. One of the main drawbacks that unfortunately limits the general usage of steel hollow sections is the physically instabilizing local buckling failures under concentrated forces. A specific example is a steel HSS column with corbel heavily supporting industry crane loads of warehouses [2]-[4]. The HSS members has made itself prone to the premature failure caused by the eccentrically applied loads.

The intrinsic behaviors of HSS undergoing local buckling phenomena are rather sporadic. These have yet been precisely described by standard mathematical formulations [5]. The design guidelines were developed in the form of empirical formulations to predict the local buckling responses of steel open sections under compression and/or flexural forces, and the strengthening procedures were made available for the enhancement of the overall member capacity. However, little is known about the behaviors and strengthening methods of the HSS applications.

The investigation of I-beam to box-column connection (IBBC) with external stiffener was reported in Ting [6] and Shanmugam [7]. The study of external T-stiffeners connected to IBBC was provided in [8]. In 2000, Hiroshi and Tanaka [9] conducted the experimental study of IBBC with external stiffener by wide spread flange. Furthermore, the numerical study of an external stiffener with IBBC was present in [10]. The work in [11] and [12] conducted experimental and numerical analyses of external diaphragm with IBBC in the concrete filled column applications. The aforementioned work adopted the strengthening techniques using external stiffening systems to facilitate the load transfer from beam to column members. The internal retrofits of HSS columns are generally inaccessible for practical constructions.

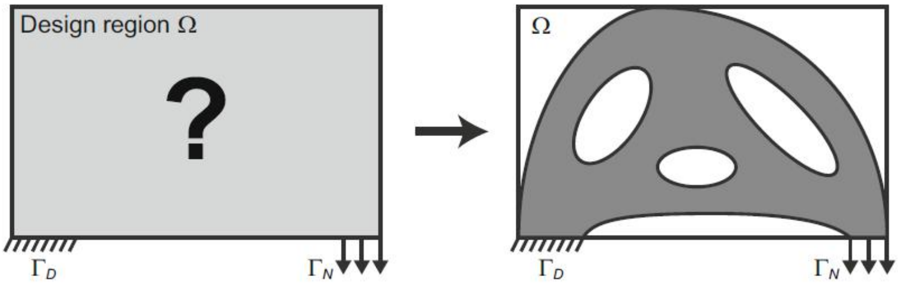

Figure 1. Illustration of typical structural topology optimization [13].

Topology Optimization (TO) determines the optimal shape as depicted in Fig. 1. The prior investigation of TO can be traced back to over a hundred years ago by Michell [14], who derived the optimality criteria of the least-weight truss layout. Mitchell's theory was extended 70 years later by Rozvany and his group [15]-[17] for the exact analytical optimal solutions of grid-type structures. In continuum mechanics, topology optimization can be formulated as a discrete problem or a binary design setting that the structure consists solely of either solids or voids [18]. However, the binary design for the structural compliance is ill-posed, where there exists non-convergent sequence of admissible designs with continuously refined geometrical details [19]-[22]. Bendsøe and Kikuchi [23] proposed the homogenization theory to relax the problem by assuming designable porous microstructures at a separated lower scale to claim this difficulty.

There has been the continuous development giving the emergence of various TO methods. One of the well-established techniques proposed by Xie and Steven [24]-[25] is called as an evolutionary structural optimization (ESO). Recently, the bi-evolutionary structural optimization (BESO) [27]-[29] has been developed. The method allows the recovery of the deleted elements close to the highly stressed areas. The convergent and mesh-independent BESO method [30] incorporates the sensitivity filter and stabilization schemes using some history information.

The present work proposes the optimal retrofit design of steel HSS columns in the IBBC region supporting heavily forces. The optimal topology of externally strengthening steel plates is appropriately designed using the BESO algorithm. The IBBC responses with and without optimal strengthening plates are mapped out by the nonlinear (incorporating inelastic materials and large deformations, simultaneously) finite element analysis method (FEM), modelled within the robust commercial-purposed (called ANSYS) analysis software. The applications of the proposed retrofit method are illustrated through the strengthening design of the HSS column connected to a corbel supporting industry crane loads.

2. Design guideline for column stiffening methods

2.1 Crane Loads

The crane load is determined according to [3] and [4]. The HSS columns are be designed to safely resist the applied loads and to prevent the local or global buckling failures. The detail of the top running cranes is depicted in Fig. 2.

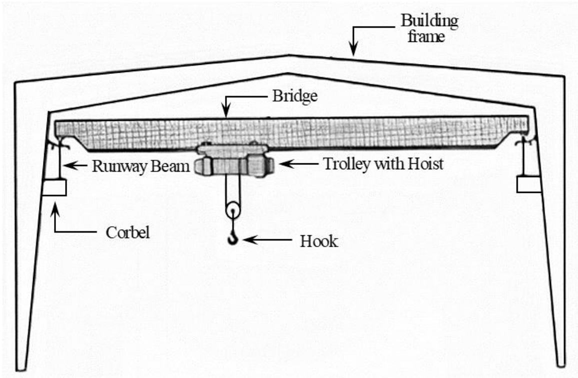

Figure 2. Top Running Bridge Crane with Suspended Trolley [3].

The model is constructed to predict the responses of the connection between HSS column and I-section corbel under the vertically applied forces. The vertical forces consider the wheel loads. The maximum magnitude occurs as when the crane is lifting its rated capacity load, and can be approximated as

$$WL = \frac{RC + HT + 0.5CW}{NW_b} \tag{1}$$

where WL is the maximum wheel load, RC is the rated crane capacity, HT is the weight of hoist with trolley, CW is the weight of the crane excluding the hoist with trolley. and NW_b is the number of end truck wheels at one end of the bridge.

2.2 External stiffener plates

The retrofit of the beam-to-column connection focuses on the local failure behaviors (viz., chord deformations [31]) of the HSS columns. The external stiffening plates are designed for this purpose. The study of the connection between I-beam and Circular Hollow Section (CHS) column with external stiffeners is reported in [32] and [33]. The geometry of the HSS columns at IBBC zone with the proposed external ring plates are illustrated in Fig. 2,

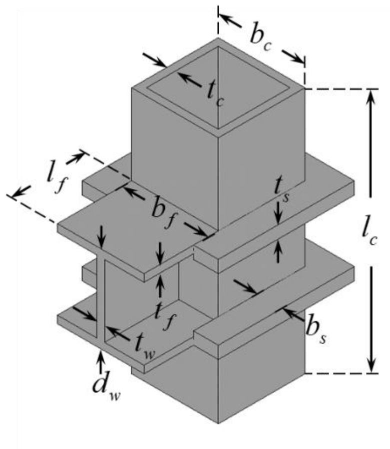

Figure 2. Geometry of IBBC with external ring plates.

where b_c is the column width, b_f and d_w are the flange width and web depth of an I-beam, respectively, t_c is the column thickness, t_f and t_w are the thickness of flange and web, respectively, t_s is the thickness of external stiffener plates, l_f is the beam length, and l_c is the volume length.

2.3 Topology optimization formulations

The topology design of stiffener plates considers the minimization of the compliance function, namely $f_c = \frac{1}{2}\mathbf{u}^T\mathbf{K}\mathbf{u}$, subject to the volume fraction constraint of the continuum model, and can be formulated by

$$\begin{aligned} &\text{Minimization} && : f_c(x, \mathbf{u}) \\ &\text{subject to} && : \mathbf{Ku} = \mathbf{F} \\ & && : V(x) = \sum_{e=1}^{N_e} x_e v_e = V^* \end{aligned} \quad , \tag{2}$$

where $\mathbf{K}$ and $\mathbf{u}$ are the global stiffness matrix and displacement vector at degrees of freedom, respectively, v_e is the element volume, $V(x)$ and V^* are the total and controlled material volumes (called volume fraction, i.e.,), respectively, N_e and x_e are the total number of finite elements and the material design variable, respectively.

The conventional ESO method known as a "hard-kill" method performs the complete elimination of some inefficient members within the design domain that can result in theoretical difficulties in some cases [34].

An alternative approach adopts the modulus reductions of the required elements to the very small values. This concept was applied to ESO by Hinton [35] and Rozvany [36]. Huang and Xie [37] replaced the virtual void elements with the soft members with very low Young's modulus values, and termed the method as a "soft-kill" BESO. This technique is an artificial material interpolation scheme with penalization that is similar to the treatment in the solid isotropic material with penalization (SIMP) model in steering the solution to the nearly solid-void design [38]-[40]. The elastic modulus of each intermediate material is interpolated as a function of the element density as

$$E(x_e) = E^0 x_e^p \text{, where } x_e = x_{\min} \text{ or } 1 \tag{3}$$

E_0 denotes the elastic modulus of a solid material, and p is the penalty exponent. The binary variable x_e indicates the absence ($x_e = x_{\min}$)or presence ($x_e = 1$) of the element, where $x_{\min}$ is an artificially defined small parameter (e.g., 0.001). It is assumed that the Poisson's ratio is independent from the design variables, and the stiffness matrix $\mathbf{K}$ assemblies the products of elemental stiffness matrices $\mathbf{K}_e^{\mathbf{0}}$ and design variables x_e^p by

$$\mathbf{K} = \sum_{e=1}^{N_e} x_e^p \mathbf{K}_e^0 . \tag{4}$$

At each design stage, the target volume in the current l-th design iteration $V^{(l)}$ is preset a priori. The required material volume can be greater or smaller than the volume of the initial guess design. Likewise, the target volume in each iteration may decrease or increase progressively until the constraint volume is achieved. The evolution of the volume is expressed by

$$V^{(l)} = V^{(l-1)}\left(1 \pm c_{er}\right), \tag{5}$$

where the evolutionary ratio c_{er} determines the percentage of material to be added or removed with reference to the design in the previous iteration. After the targeted material volume V_{req} has been attained, the optimization alters only the topology whilst keeping the volume constant (up to a certain tolerance). The sensitivity of the structural compliance with regards to the change in the *e*-th element is evaluated by the adjoint function [41] as

$$\frac{\partial f_c}{\partial x_e} = -p x_e^{p-1}\left(\frac{1}{2}\mathbf{u}_e^T \mathbf{K}_e^0 \mathbf{u}_e\right), \tag{6}$$

where $\mathbf{u}_e$ denote elemental displacement vectors. The structure is optimized using the discrete x_e design variables, and only two bound materials are allowed in the design [18]. Therefore, the sensitivity number used in the BESO method is defined by the relative ranking of the sensitivity associated with the individual element as

$$\alpha_e = -\frac{1}{p}\frac{\partial f_c}{\partial x_e} = x_e^{p-1}\left(\frac{1}{2}\mathbf{u}_e^T \mathbf{K}_e^0 \mathbf{u}_e\right). \tag{7}$$

In order to avoid checkerboard patterns and mesh-dependency, the sensitivity numbers are firstly smoothed by means of the filter scheme as

$$\alpha_e = \frac{\sum_{j=1}^{N_e} w_{ej}\alpha_j}{\sum_{j=1}^{N_e} w_{ej}}, \tag{8}$$

where w_{ej} is a linear weight factor computed by the prescribed filter radius $r_{\min}$ and the elemental center-to-center distance Δ_{ej} between elements Ω_e and Ω_j as

$$w_{ej} = \max\left(0, r_{\min} - \Delta_{ej}\right). \tag{9}$$

The filtered sensitivity numbers are averaged with the sensitivity numbers of the previous topology iteration to improve the convergence by

$$\alpha_e^{(l)} = \left(\alpha_e^{(l)} + \alpha_e^{(l-1)}\right)/2. \tag{10}$$

The BESO algorithm optimizes the structure by removing and adding the elements assigned in the ground domain. Two discrete values, namely $x_{\min}$ for void elements and 1 for solid elements, are applied [42]. The sensitivity numbers for the solid and void elements are expressed by

$$\alpha_e = \begin{cases} \frac{1}{2}\mathbf{u}_e^T \mathbf{K}_e^0 \mathbf{u}_e & \text{when } x_e = 1 \\ x_{\min}^{p-1}\left(\frac{1}{2}\mathbf{u}_e^T \mathbf{K}_e^0 \mathbf{u}_e\right) & \text{when } x_e = x_{\min} \end{cases}. \tag{11}$$

The sensitivity numbers of solid elements are independent to the penalty exponent p, whilst those numbers of the soft elements depend on the p value.

The recent BESO approach has been developed to the optimal topology for a wide range of structural design applications, involving multiple materials [37], multiple constraints [43], stiffness and frequency optimization [44] and nonlinear material and large deformation [45]-[48]. The present plate strengthening approach proposed adopts the BESO algorithm, and the procedures as how the optimal retrofit design is performed are described in Section 3.

3. Analysis and design of column stiffening

3.1 Traditional Retrofit design

The responses of steel HSS columns (over an IBBC area) under crane loads were mapped out using the nonlinear 3D finite element (FE) analyses. The SHS - 300 × 10 ($b_c \times t_c$) columns were considered as for illustrative purposes. The standard steel corbels H - 300 × 300 × 10 × 10 ($b_f \times d_w \times t_f \times t_w$) were employed, where the length of column l_c and corbel l_f equal to 1 m and 300 mm respectively. The analyses considered the responses of stiffened HSS columns for various plate thicknesses t_s, ranging from 3 to 10, 15 and 30 mm. The external ring stiffeners having a typical width of $b_s = 100$ mm.

The commercial purposed ANSYS Parametric Design Language (APDL) software modeled the structure as a number of (uniform 10 mm in size) eight-node solid (SOLID185) FEs (see Fig. 3). The HSS column was restrained in all directions at both ends, except that the deformation along a z-axis direction was released at the top end to permit its vertical translation under applied forces. The material properties employed were: the elastic modulus of 200,000 MPa, Poisson's ratio of 0.3 and yield stress of 235 MPa (for both column and beam) and 250 MPa (for the stiffening plate).

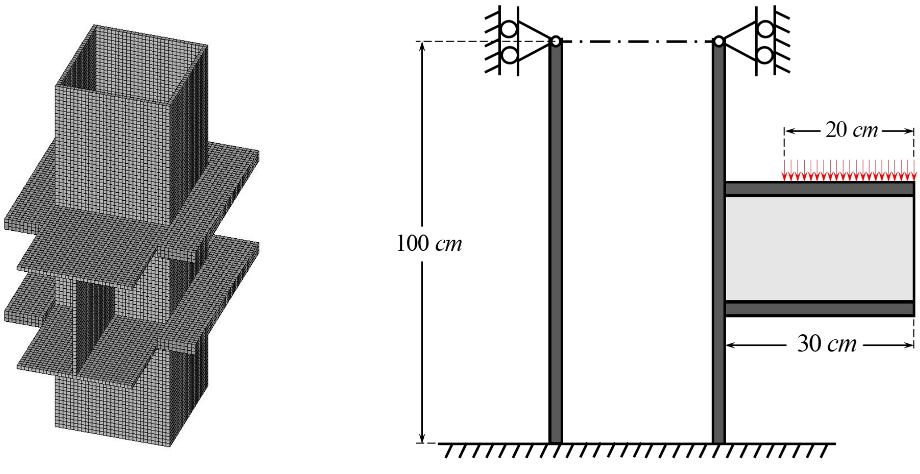

(a) (b)

Figure 3. Structural discretization (a) FE model and (b) boundary conditions.

The FE analyses incorporated the influences of inelastic (elastic-perfectly plastic) materials and large (nonlinear geometry) deformations to realistically map out the full responses of the HSS column at an IBBC zone. The crane load was applied over a 20 cm width contact surface on an I-section corbel (see Fig. 3b).

3.2 BESO algorithm procedure

The topology of the two HSS column stiffening plates located at the top and bottom flanges of an I-beam were designed using the BESO algorithm [27]-[29]. The design procedures can be briefly summarized as follows:

Step 1: Discretize the design domain as in Fig. 3a with the sufficient number of eight-node solid (SOLID185) FEs. The domain initially sets the thickness of stiffener plates to $t_s = 30$ mm.

Step 2: Initialize the BESO parameters, including objective volume V^*, evolutionary ratio c_{er}, radius of filter $r_{\min}$ and penalty exponent p.

Step 3: Perform the nonlinear FE analyses. Only the two stiffening plates are designed by the BESO schemes.

Step 4: Determine the targeted volume in Eq. (5) for the next iteration, if the current volume $V^{(l)}$ is larger than the objective volume V^*.

Step 6: Calculate the sensitivity functions in Eq. (8).

Step 7: Perform the elimination and addition process. The elemental density is switched from 1 to $x_{\min}$ (i.e., a member addition) if $\alpha_e \leq \alpha_{th}$. In contrast, the elemental density for void element is switched from $x_{\min}$ to 1 (member elimination) if $\alpha_e > \alpha_{th}$. The threshold α_{th} defines the threshold on the sensitivity number that is determined by the target material volume $V^{(l+1)}$and the relative ranking of the sensitivity numbers, see [30].

Step 8: Repeat Steps 3 to 7. The algorithm terminates when the optimal topology of steel stiffening plates is converged.

It is noted that this work investigated the variation of the optimal plate topologies for different values of V^*, namely ranging from 0.5 down to 0.05 (e.g., indicating only 5 percent of initial design elements were remained in the final solutions). The responses of a HSS column with the resulting stiffening plates at an IBBC area were traced by the elastoplastic analyses in an ANSYS software to ensure the safety and integrity of the solutions.

4. Results and Discussions

The BESO method were successfully performed to achieve the optimal solution. The resulting optimal topologies of stiffening plates for difference volume fraction V^* are depicted in Fig. 5. The full responses of the HSS columns with designed retrofitting steel plates at an IBBC zone were traced by performing the nonlinear material and geometry FE analyses. The corresponding maximum load capacities for all the designed cases are reported in Table 1. Clearly, the higher volume fractions V^* yielded the stronger HSS columns retrofitted and hence the IBBC behaviours giving the capability to support the heavier crane loads applied on the I-section corbel.

The simple design was also performed for the ring plates in Fig. 2 with both top and bottom ring plates having the uniform thickness varying from $t_s = 3$ mm to 30 mm (without the BESO implementation). The maximum load capacities of the corresponding HSS columns at the IBBC zone captured by the comprehensive FE analyses are reported in Table 2 and are directly compared in Fig. 6 with those obtained after the retrofitting designs using the BESO method. The results obviously shown the volume fractions V^* 0.1, 0.2, 0.3 and 0.5 have more maximum load capacities than t_s 3, 6, 9 and 15 mm around 33.8, 25.59, 18.55 and 5.92 %. It is evidenced that at the same volume of designed external plates the strength gained by the BESO process is more than that by the uniform plate thickness retrofits. The BESO provided significantly the effective plate strengthening designs of the HSS columns at the IBBC area with the high value of strength enhancement per unit volume of the plates employed.

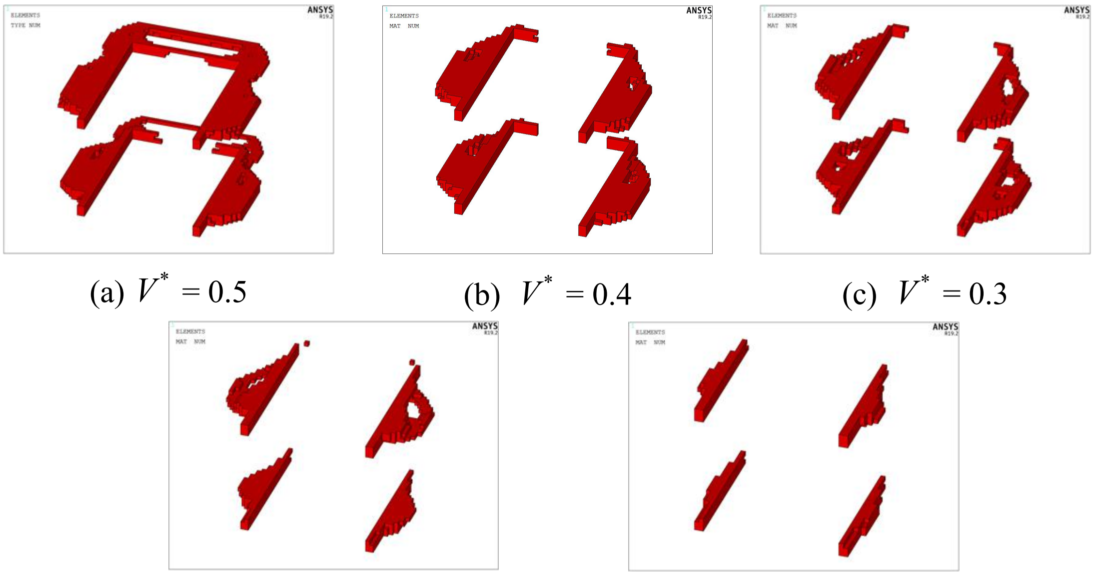

(a) $V^* = 0.5$ (b) $V^* = 0.4$ (c) $V^* = 0.3$

(d) $V^* = 0.2$ (e) $V^* = 0.1$

Figure 5. Optimal solution with different objective volume.

Table 1. Maximum load capacities for various design volumes by BESO.

V^*	Volume (cm^3)	P_{NL} (Tons)
0.05	390	82.450
0.10	780	91.305
0.15	1,170	95.858
0.20	1,560	98.126
0.25	1,950	99.872
0.30	2,340	105.220
0.35	2,730	105.420
0.40	3,120	107.290
0.45	3,510	110.760
0.50	3,900	113.600

Table 2. Maximum load capacities for various design volumes by uniform-thickness plate design.

t_s (mm)	Volume (cm^3)	P_{NL} (Tons)
unstiffened	–	58.487
3	780	68.146
4	1,040	71.508
5	1,300	74.907

6	1,560	78.319
7	1,820	81.749
8	2,080	85.220
9	2,340	88.753
10	2,600	91.888
15	3,900	107.890
30	7,800	126.690

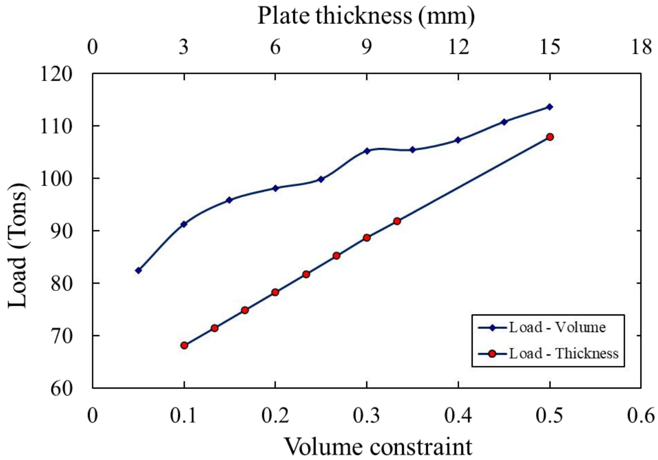

Figure 6. Maximum load capacities with different techniques.

5. Concluding remarks

This paper presents the steel plate topology optimization for the strengthening design of HSS columns at an IBBC zone subjected to the industry crane loads. The initial design domains are the thick ring-shape steel plates enveloping the HSS column at the contacts on top and bottom flanges of the I-section corbel. The BESO method has been developed for the determination of optimal material distributions through the process of a soft-kill optimization, permitting not only elimination but also addition of steel masses for various targeted volume fractions. The influences of inelastic material as well as local steel buckling failures are incorporated using the comprehensive nonlinear material and geometry FE analyses.

The optimal topology of the retrofitting plates computed provides the maximum strength enhancement to the HSS columns at the IBBC area, whilst the associated design volumes are maintained the indicated fractions. The efficiency of the BESO method has been evidenced, where the maximum load capacities of the HSS columns retrofitted by the steel plates with the optimal layouts in the IBBC can be achieved at the far lower plate volumes, as compared to those with the simple uniform-thickness plate designs. Extensions to the present work focus on the applications of steel open-section columns having different slenderness practically employed in engineering structures.

6. Acknowledgements

This research has been supported under the Thailand Research Fund (Grant No. RSA6280089). The financial support provided by Chulalongkorn University under Ratchadaphiseksomphot Endowment Fund and Second Century Fund is acknowledged.

References

[1] Kurobane, Y., Packer, J.A., Wardenier, J. (2004) Design guide for structural hollow section column connections. CIDECT Series "Construction with hollow steel sections" No. 9, TÜV-Verlag, Köln, Germany, ISBN 3- 8249-0802-6.

[2] Maccrimmon, R. (2009) Crane-Supporting Steel Structure. 2nd Edition. Canadian Institute of Steel Construction, Niagara Falls, Ontario, Canada.

[3] MBMA (2012) Metal Building Systems Manual, based on the 2012 IBC and ASCE 7-10, Cleveland, Ohio.

[4] NBCC (2015) National Building Code of Canada, Ottawa: Associate Committee on the National Building Code, National Research Council.

[5] Lu, L. H. (1997). The static strength of I-beam to rectangular hollow section column connections. Ph.D. Dissertation, Delft University, Netherlands.

[6] Ting, L. C., Shanmugam, N.E., Lee, S.L. (1991). Box-column to I-beam connections with external stiffeners. *Journal of Constructional Steel Research* **18,** (3): 209-226.

[7] Shanmugam, N.E., Ting, L. C., Lee, S.L. (1993) Static behaviour of I-beam to box-column connections with external stiffeners. *The Structural Engineer* **71,** (15): 269–275.

[8] Ting, L. C., Shanmugam, N.E., Lee, S.L. (1993). Use of external T-stiffeners in box-column to I-beam connections. *Journal of Constructional Steel Research* **26,** (2-3): 77–98.

[9] Hiroshi, M., and Tanaka, A. (2000). Statical characteristics of the improved beam-to-column connections of steel structure. *Proceedings of 12th World Conference on Earthquake Engineering*, Auckland, New Zealand.

[10] Goswami, R., Murty, C. V. R. (2010). Externally Reinforced Welded I-Beam-to-Box-Column Seismic Connection. *Journal of Engineering Mechanics* **136**, (1): 23–30.

[11] Vulcu, C., Stratan, A., Ciutina, A., and Dubina, D. (2017a). Beam-to-CFT High-Strength Joints with External Diaphragm. I: Design and Experimental Validation. *Journal of Structural Engineering* **143**, (5).

[12] Vulcu, C., Stratan, A., Ciutina, A., and Dubina, D. (2017b). Beam-to-CFT High-Strength Joints with External Diaphragm. II Numerical Simulation of Joint Behavior. *Journal of Structural Engineering* **143,** (5).

[13] Xia, L., & Breitkopf, P. (2016). Recent Advances on Topology Optimization of Multiscale Nonlinear Structures. *Archives of Computational Methods in Engineering* **24**, (2): 227–249.

[14] Michell, A. G. M. (1904) Lviii. the limits of economy of material in frame-structures. *The London, Edinburgh, and Dublin Philosophical Magazine and Journal of Science* **8**, (47): 589–597.

[15] Prager, W., Rozvany, G. (1977) Optimal layout of grillages. *Journal of Structural Mechanics* **5**, (1): 1–18.

[16] Rozvany, G. (1972) Grillages of maximum strength and maximum stiffness. *International Journal of Mechanical Sciences* **14**, (10): 651–666.

[17] Rozvany, G. (1972) Optimal load transmission by flexure. *Computer Methods in Applied Mechanics and Engineering* **1**, (3): 253–263.

[18] Xia, L., Xia, Q., Huang, X., and Xie, Y. M. (2016). Bi-directional Evolutionary Structural Optimization on Advanced Structures and Materials: A Comprehensive Review. *Archives of Computational Methods in Engineering* **25**, (2): 437–478.

[19] Cheng, K., Olhoff, N. (1981) An investigation concerning optimal design of solid elastic plates. *International Journal of Solids and Structures* **17**, (3): 305–323.

[20] Kohn, R., Strang, G. (1986a) Optimal design and relaxation of variational problems (part i). *Commun Pure Applied Math* **39**, (1): 113–137.

[21] Kohn, R., Strang, G. (1986b) Optimal design and relaxation of variational problems (part ii). *Commun Pure Applied Math* **39**, (2): 139–182.

[22] Kohn, R., Strang, G. (1986c) Optimal design and relaxation of variational problems (part iii). *Commun Pure Applied Math* **39**, (3): 353–377.

[23] Bendsøe, M. P., & Kikuchi, N. (1988). Generating optimal topologies in structural design using a homogenization method. *Computer Methods in Applied Mechanics and Engineering*, **71,** (2): 197–224.

[24] Xie, Y. M., Steven, G.P. (1992) Shape and layout optimization via an evolutionary procedure. *In: Proceedings of the International Conference on Computational Engineering Science*, Hongkong, China.

[25] Xie, Y. M., Steven, G.P. (1993) A simple evolutionary procedure for structural optimization. *Computers and Structures* **49**, (5): 885-896.

[26] Xie, Y. M., Steven, G.P. (1997) Evolutionary Structural Optimization. Springer-Verlag, London.

[27] Querin, O. M., Steven, G. P., and Xie, Y. M. (1998). Evolutionary structural optimisation (ESO) using a bidirectional algorithm. *Engineering Computations* **15**, (8): 1031–1048.

[28] Querin, O. M., Steven, G. P., and Xie, Y. M. (2000) Evolutionary structural optimization using an additive algorithm. *Finite Elements in Analysis and Design* **34**, (3): 291–308.

[29] Querin, O. M., Young, V., Steven, G. P., and Xie, Y. M. (2000). Computational efficiency and validation of bi-directional evolutionary structural optimisation. *Computer Methods in Applied Mechanics and Engineering* **189**, (2): 559–573.

[30] Huang, X., and Xie, Y. M. (2007). Convergent and mesh-independent solutions for the bi-directional evolutionary structural optimization method. *Finite Elements in Analysis and Design* **43**, (14): 1039–1049.

[31] Lee, M. M., and Llewelyn-Parry, A. (1999). Strength of ring-stiffened tubular T-joints in offshore structures. *Journal of Constructional Steel Research* **51**, (3): 239–264.

[32] Bagheri Sabbagh, A., Chan, T. M., and Mottram, J. T. (2013). Detailing of I-beam-to-CHS column joints with external diaphragm plates for seismic actions. *Journal of Constructional Steel Research* **88**: 21–33.
[33] Tritep, U. and Kitjapat, P. (2016). Strength Enhancement of Connections between Steel I-Beam and Circular Hollow Steel Column by Nonlinear Finite Element Analysis. *National Convention on Civil Engineering (NCCE21)*, Songkla, Thailand, 28-30 June 2016, pp.35-43.
[34] Zhou, M., and Rozvany, G. I. N. (2001). On the validity of ESO type methods in topology optimization. *Structural and Multidisciplinary Optimization* **21**, (1): 80–83.
[35] Hinton, E., and Sienz, J. (1995). Fully stressed topological design of structures using an evolutionary procedure. *Engineering Computations* **12**, (3): 229–244.
[36] Rozvany, G. I. N., and Querin, O. M. (2002). Combining ESO with rigorous optimality criteria. *International Journal of Vehicle Design* **28,** (4): 294.
[37] Huang, X., and Xie, Y. M. (2008). Bi-directional evolutionary topology optimization of continuum structures with one or multiple materials. *Computational Mechanics* **43**, (3): 393–401.
[38] Bendsøe, M. P. (1989). Optimal shape design as a material distribution problem. *Structural Optimization* **1**, (4): 193–202.
[39] Bendsøe, M. P., and Sigmund, O. (1999). Material interpolation schemes in topology optimization. *Archive of Applied Mechanics (Ingenieur Archiv)* **69**, (9-10): 635–654.
[40] Rietz, A. (2001). Sufficiency of a finite exponent in SIMP (power law) methods. *Structural and Multidisciplinary Optimization* **21**, (2): 159–163.
[41] Bendsøe, M. P. and Sigmund, O. (2003) Topology optimization: theory, methods and applications. Springer-Verlag, Berlin.
[42] Huang, X., and Xie, Y. M. (2007). Convergent and mesh-independent solutions for the bi-directional evolutionary structural optimization method. *Finite Elements in Analysis and Design* **43**, (14): 1039–1049.
[43] Huang, X., and Xie, Y. M. (2009). Evolutionary topology optimization of continuum structures with an additional displacement constraint. *Structural and Multidisciplinary Optimization* **40**, (1-6): 409–416.
[44] Huang, X., Zuo, Z. H., and Xie, Y. M. (2010). Evolutionary topological optimization of vibrating continuum structures for natural frequencies. *Computers and Structures* **88**, (5-6): 357–364.
[45] Huang, X. H., and Xie, Y. (2007). Bidirectional Evolutionary Topology Optimization for Structures with Geometrical and Material Nonlinearities. *AIAA Journal* **45**, (1): 308–313.
[46] Huang, X., and Xie, Y. M. (2008). Topology optimization of nonlinear structures under displacement loading. *Engineering Structures* **30**, (7): 2057–2068.
[47] Huang, X., and Xie, Y.-M. (2010). A further review of ESO type methods for topology optimization. *Structural and Multidisciplinary Optimization* **41**, (5): 671–683.
[48] Xia, L. (2016) Multiscale structural topology optimization. Elsevier-ISTE, London.